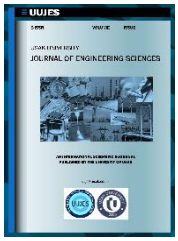

Usak University

Journal of Engineering Sciences

An international e-journal published by the University of Usak

Journal homepage: dergipark.gov.tr/uujes

Research article

EXPLORING THE INFLUENCE OF B-SITE DOPANTS ON STRUCTURAL AND MAGNETIC PROPERIES IN $La_{0.8}Ag_{0.2}Mn_{1-x}Co_xO_3$ (x: 0 and 0.1) COMPOUNDS

Barış Altan[1,2], Yavuz Selim Ak[2], Atilla Coşkun[2]*

[1]Department of Medical Imaging Techniques, Vacational School of Health Services, Fenerbahçe University, İstanbul, Türkiye
[2]Department of Physics, Faculty of Sciences, Muğla Sıtkı Koçman University, Muğla, Türkiye

Received: 28 May 2024 Revised: 06 June 2020 Accepted: 10 June 2024 Online available: 30 June 2024

Abstract

This study examines the structural, electrical, magnetic, and magnetocaloric properties of $La_{0.8}Ag_{0.2}Mn_{0.9}A_{0.1}O_3$ (A: Mn, and Co) compounds under doping in the B-site. XRD results show that the compound containing Co ions directly replaced Mn ions in the B-site without forming a secondary phase containing higher metallic Ag impurities. The data obtained using Scanning electron microscopy with energy dispersive X-ray spectroscopy (SEM-EDS), the temperature dependence of magnetization (M-T), the magnetic field dependence of magnetization (M-H), and the magnetic entropy change (ΔS_M) analysis reveal the effect of the doped element on the magnetic properties of the compounds due to the changes they create in the structural and Mn^{3+}/Mn^{4+} ratio. It has been determined that the paramagnetic to ferromagnetic transition temperature (Curie temperature, T_C) of the $La_{0.8}Ag_{0.2}Mn_{0.9}Co_{0.1}O_3$ (LAMO-Co) is quite lower than the LAMO.

Keywords: *Magnetocaloric effect; Sol-gel; XRD Refinement; Curie Temperature; Composite materials; Perovskite.*

1. Introduction

The magnetocaloric effect, known for altering a material's temperature when subjected to a magnetic field, has gained substantial interest due to its potential to enhance refrigeration and cooling systems [1-3]. This effect presents a hopeful path toward boosting the efficiency and eco-friendliness of refrigeration technologies, driving ongoing

*Corresponding author: Atilla Coşkun
E-mail: acoskun@mu.edu.tr (ORCID: 0000-0002-6695-0696)
DOI: 10.47137/uujes.1491191

research and development efforts. Recent studies have revealed that manganite compounds in ABO_3 perovskite structure [4-7], which exhibit magnetocaloric properties, may be promising candidates to replace Gd-based alloys [8-10] due to their unique magnetic and structural properties. These compounds exhibit versatile applications across various technological domains, including magnetic refrigeration, solid-state cooling devices, and magnetic sensors [11, 12]. The ability to fine-tune their properties through dopant additions in both the A and B-sites of the perovskite lattice further enhances their suitability for specific applications. The optimization of the T_C of manganite compounds for practical applications near room temperature frequently entails adjusting the Mn^{3+}/ Mn^{4+} ratios. The Mn^{3+}/ Mn^{4+} ratios in manganite compounds are often influenced by dopant additions in the A-site [13, 14]. These dopants play a crucial role in modulating the relative proportions of Mn^{3+} and Mn^{4+} ions' valence states, thereby affecting the compounds' magnetic and structural properties [15-17]. Additionally, the substitution of Mn ions in the B-site with transition metal dopants introduces various changes, reflecting the importance of understanding the valency of the contributing elements [18–20]. Studies investigating the replacement of some Mn ions in the B-site of manganite compounds with dopant elements such as Cu, Ni, Fe, and Co have revealed conflicting results. For instance, one study reported that entering Cu elements instead of some Mn ions into the B-site resulted in Cu ions adopting a 2+ valence state within the crystal structure [21]. In contrast, another study revealed that Cu ions settled in the B-site of the perovskite structure with a 3+ valence [22]. Additionally, another study suggests that Cu ions coexist in both 2+ and 3+ valence states within the crystal lattice [23]. As a result, the discrepancies in these studies make it challenging to definitively determine the valence state of the dopant element in the crystal structure when replacing some of the Mn ions in the B-site. As can be understood, the lack of precise information regarding the exact value of valency of dopant elements in the B-site has hindered accurate interpretations of experimental results and limited the development of tailored manganite materials.

The compound $La_{0.8}Ag_{0.2}MnO_3$, as a member of the manganite family, provides an example of the perovskite structure, and this structure is the source of important physical properties that are used in different technological applications, such as high magnetic entropy changes and colossal magnetoresistance. The stability and magnetic properties of the crystal structure can change significantly under the influence of doping, especially in the Mn substitution in the B-site. These additives can affect the structural and electronic properties of manganite compounds, leading to magnetic phase transitions, and changes in electronic structure at critical temperatures. Therefore, doping of the Mn substitution in the B-site has an important role in controlling the fundamental magnetic properties of manganite compounds. In this study, this study aims to deeply examine the effect of doping with the Co element, constituting 10% of the $La_{0.8}Ag_{0.2}MnO_3$ compound, instead of Mn, on its structural, magnetic, and electronic properties. Through this investigation, we targeted to obtain valuable insights into the fundamental physical properties of manganite compounds and their potential applications.

2. Experimental Details

The synthesis of the $La_{0.8}Ag_{0.2}Mn_{1-x}Co_xO_3$ (x: 0 and 0.1) compounds was carried out via the sol-gel technique, wherein the solid precursor obtained underwent thorough grinding to ensure homogeneity. Instead of detailing the experimental procedure, we prefer to reference our previously published article [24]. The samples were sintered at 1000 ^oC for 24 hours in air and then cooled to room temperature in the furnace. In this paper, for the sake of simplicity, we utilize abbreviated composite names as follows: $La_{0.8}Ag_{0.2}MnO_3$ is denoted as LAMO, $La_{0.8}Ag_{0.2}Mn_{0.9}Co_{0.1}O_3$ is abbreviated as LAMO-Co. The X-ray diffraction

(XRD) measurements of the compounds were carried out in the 2θ range of 10-100 degrees. XRD analyses were performed to elucidate parameters such as space group, crystal structure parameters, Mn-O bond lengths, Mn-O-Mn bond angles, and other structural features of the compounds. In addition, Rietveld refinements were performed using the FullProf program to accurately determine these parameters. Surface imaging operations were conducted using the JEOL 7600F model high-resolution SEM to revealing the morphologies, grain sizes, and grain formations on the surface of the compounds. Concurrently, Energy Dispersive X-ray Spectroscopy (EDS) studies were performed during the SEM analyses to determine the elemental composition and distribution in the samples. The Physical Property Measurement System (PPMS) Quantum Design DynaCool-9 was used to explore the magnetic properties of samples. This advanced apparatus operates within a controlled temperature range changing from 1.8 K to 400 K. Furthermore, this configuration affords the precise application of magnetic fields, spanning from 0 T to 5 T, thereby allowing comprehensive investigation of magnetic behaviors of materials. The investigation includes magnetization measurements as a function of both temperature and magnetic field, denoted as M-T and M-H, respectively. The measurements of M-T were conducted under various modes including zero field cooling (ZFC), field cooling (FC), and field heating (FH), employing a magnetic field strength of 50 mT. This comprehensive procedure spanned temperatures from 5 K to 380 K. The M-H measurements were performed above and below their T_C, at certain temperatures with 4 K intervals, and by applying a magnetic field from 0 to 5 T. Isothermal M-H curves were used to calculate the magnetocaloric effect ($-\Delta S_M$) of the compounds, and the physical equations on which these calculations are based are explained in [21].

3. Results and Discussions

3.1. XRD analysis

XRD analyses were conducted to determine the crystal structure properties of the compounds. The crystal structure parameters of the compounds were determined through XRD analyses, utilizing Rietveld refinement in conjunction with the Fullprof program. This integrated methodology facilitated the precise determination of crystal structure parameters, including Mn-O bond lengths and Mn-O-Mn bond angles, as well as encompassing unit cell dimensions, atomic coordinates, and phase compositions. Fig.1(a-b) illustrates the refined XRD patterns of the compounds following the Rietveld refinement process. The detailed analysis of crystal structure parameters for all compounds is presented in Table 1. As a result of XRD analyses, it was determined that LAMO, and LAMO-Co compounds crystallize in a perovskite structure, and each includes different volumetric ratios of metallic silver impurities. Particularly in Ag-doped manganite compounds, including this study, there are studies in the literature indicating that depending on factors such as doping amount and thermal treatment temperature, some metallic silver segregates from the perovskite structure [25,26]. Additionally, it has been determined that LAMO, and LAMO-Co compounds have a rhombohedral structure and belong to the $R\bar{3}c$ space group, indicating that no structural transformation occurs because of doping into the B-site. Based on the information provided in Table 1, it is evident that LAMO contains fewer metallic silver impurities compared to the LAMO-Co. Consequently, since each silver ion incorporated into the perovskite structure leads to the conversion of two Mn^{3+} ions to Mn^{4+} ions, it can be inferred that LAMO-Co is likely to possess fewer Mn^{4+} ions compared to LAMO. The deficiency of silver is expected to reduce the compounds' magnetic properties. Compounds containing perovskite structures with varying, yet closely comparable volumetric ratios, have minor alterations in crystal lattice parameters, Mn-O bond lengths, and Mn-O-Mn bond angles. These changes are believed to be correlated with the number

of Ag ions present in different proportions within the perovskite structure, particularly with the substitution of Mn ions in the B-site by doping elements. This speculation arises from the varying valences of these elements, which may lead to the possibility of octahedral deformation within the crystal structure due to changes in their ionic radii corresponding

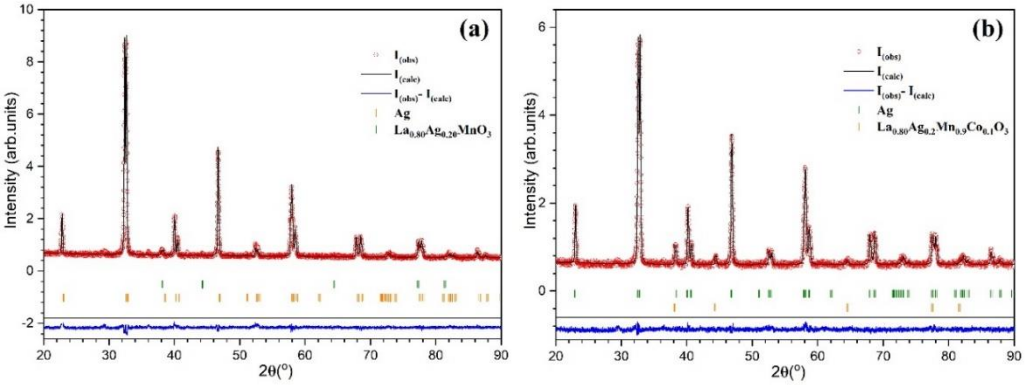

to their valence states.

Fig. 1 Observed and calculated XRD data and Rietveld refinement for a) LAMO, b) LAMO-Co

Table 1 The structural parameters were obtained from the Rietveld refinement of the samples.

	LAMO	**LAMO-Co**
Crystal Structure	Trigonal	Trigonal
Space Group	R$\bar{3}$c	R$\bar{3}$c
a(Å)	5.5171	5.5188
b(Å)	5.5171	5.5188
c(Å)	13.3495	13.3335
V(Å)^3	351.995	351.691
Mn-O-Mn (°)	160.80(3)	162.074(3)
Mn-O1 (Å)	1.9703(8)	1.9663(4)
GoF	1.2	1.1
χ^2	1.89	1.22
Phase Fract (%)	97.44	96.82
Impurities	**Ag**	**Ag**
Crystal Structure	Fm3m	Fm3m
Space Group	Cubic	Cubic
a(Å)	4.1014	4.0845
b(Å)	4.1014	4.0845
c(Å)	4.1014	4.0845
V(Å)^3	68.9923	68.1418
Phase Fract (%)	2.56	3.18

3.2. SEM analysis

SEM studies were conducted to reveal the surface morphologies, grain structures, average grain sizes, and grain formations of the compounds. SEM images of the compounds are provided in Fig. 2(a-b). It was revealed that the surface morphologies of LAMO and LAMO-Co compounds are significantly same. Based on the XRD analyses, it was found that Co ions are incorporated into the perovskite structure in the B-site doping of the LAMO compound. Additionally, SEM analyses revealed that these compounds exhibit surface morphologies similar to that of the LAMO compound suggesting that the incorporation of Co ions did not significantly alter the surface characteristics except average grain sizes. The average grain size of the LAMO compound was calculated as 409.8 nm, and that of the LAMO-Co compound was calculated as 642.4 nm.

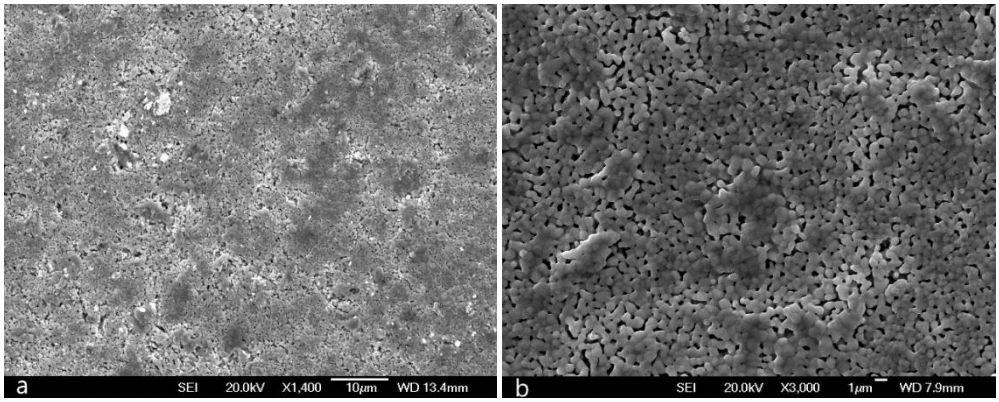

Fig. 2 The SEM images of a) LAMO, b) LAMO-Co compounds

3.3. EDS analysis

EDS serves not only to compare the chemical compositions of the targeted and produced compounds but also as a tool to unveil the presence of distinct phases within the compound. This comprehensive approach allows us to collect information on the composition of the chemical structure and serves as a kind of confirmatory of the findings found by XRD refinement within the compound and revealed by SEM analysis. Furthermore, EDS analysis, as illustrated in Fig. 3(a-b), provided the calculation of approximate chemical formulas of the phases formed in the compounds using data collected from specific points on their surfaces, although these calculations are not definitive. These calculated formulas, along with histograms obtained from SEM images and the weight percentages of elements, were provided, with the computed formulas written in the bottom right corner of each image. One notable observation in the EDS analyses was the presence of Ag ions in LAMO-Co almost at half the expected concentration. These findings are consistent with the results of XRD refinement of the LAMO-Co compound. It was revealed that the LAMO parent compound is the most stable, exhibiting

a chemical composition remarkably close to the targeted compound and demonstrating the highest stability among all the compounds studied.

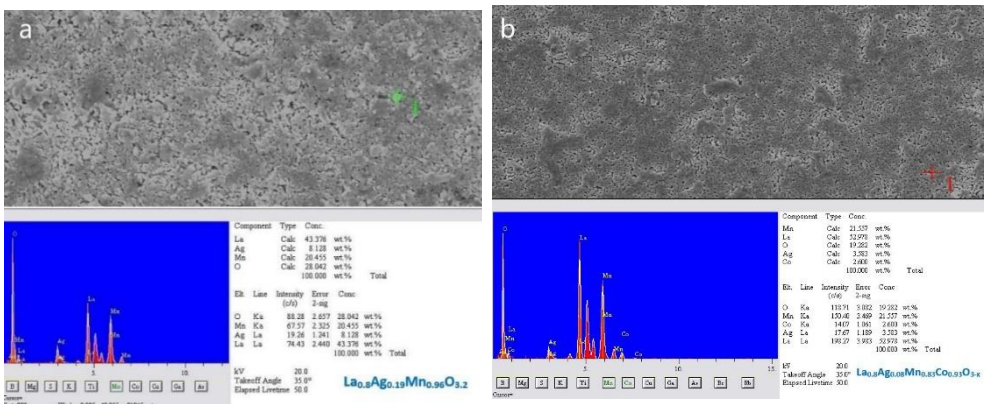

Fig. 3 EDS spectra of a) LAMO, b) LAMO-Co compoıunds

3.4. Magnetic properties

M-T analyses of the compounds were carried out to understand their magnetic properties and we especially focused on investigating the effect of doping to the B-site on the transition temperature, T_C, and magnetocaloric effect. Fig. 4(a-b) displays the temperature-dependent magnetization behavior under zero-field cooling (ZFC) and field cooling (FC) conditions for the LAMO, LAMO-Co compounds. The T_C value of the LAMO compound was found to be 289 K. This result is consistent with values reported in other studies in the literature, although some studies have reported values both below and above this range [27-29]. These variations are believed to stem from the presence of metallic Ag impurity phases within the compounds. This impurity can influence the magnetic and electrical properties of the compound, leading to different T_C values. The *Tc* value was found to be 171.2 K in the LAMO-Co sample (Fig. 4b). Structural analysis revealed that Co doping in the B-site of this sample did not lead to the formation of a secondary phase in the compound, yet the compound contained a high amount of metallic Ag impurity. Consequently, due to Ag not incorporating into the perovskite structure, there will be fewer Mn^{4+} ions and more Mn^{3+} ions formed in the perovskite structure of the compound. Therefore, depending on the valence of the Co ions in the B-site, the magnetic interactions among ions with different ratios and valences will significantly influence the magnetic properties. If the 2+ valent Co ions enter within the perovskite structure, an increase in the number of Mn^{4+} ions will occur. The 2+ valent Co ions in the perovskite structure will engage in antiferromagnetic super-exchange interactions both with each other and with Mn^{3+} (Co^{2+}-O-Mn^{3+}) and Mn^{4+} ions (Co^{2+}-O-Mn^{4+}) [30]. Similarly, if the Co ions settle into the perovskite structure with a 3+ valency, the magnetic interactions, both among themselves (Co^{3+}-O-Co^{3+}) and with Mn^{4+} ions (Co^{3+}-O-Mn^{4+}), will result in antiferromagnetic super-exchange interactions [31,32]. Ultimately, regardless of the valency of the Co ions within the perovskite structure, this will lead to an increase in antiferromagnetic interactions within the compound. This outcome explains why the T_C value of the LAMO-Co compound is significantly low.

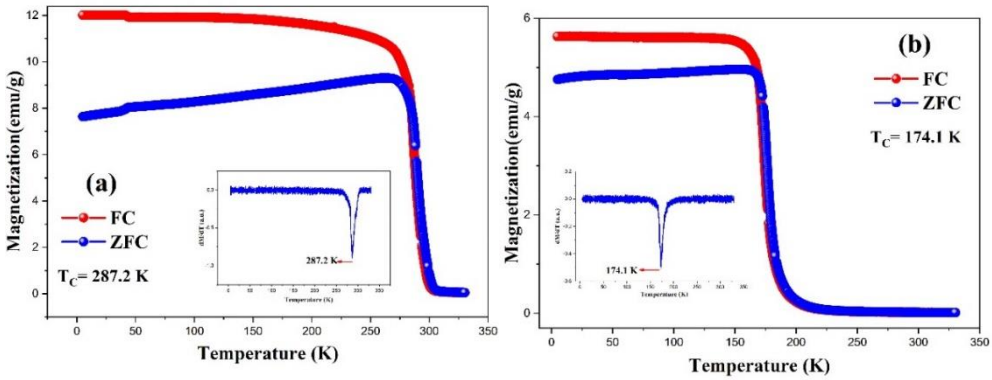

Fig. 4 The M-T curves of a) LAMO, b) LAMO-Co compound

4. Conclusion

This study was focused on investigating the structural, and magnetic properties of LAMO-based compounds doped with Co ions in the B-site. Through the comprehensive analyses, it was found that doping in the B-site significantly influences the structural and magnetic properties of these compounds. As a result of doping in the B-site, it was revealed through both XRD and SEM-EDS analyses that Co ions are incorporated into the perovskite structure of the LAMO compound. Additionally, it was determined that all compounds examined in the study contain different amounts of metallic silver impurity. It was observed that compounds incorporating Co ions in the B-site, thus directly replacing Mn ions without forming secondary phases, exhibited higher levels of metallic Ag impurities. Consequently, this implies that there will be fewer Mn^{4+} ions formed within all compounds than originally targeted. It has been determined that the paramagnetic to ferromagnetic transition temperature of the $La_{0.8}Ag_{0.2}Mn_{0.9}Co_{0.1}O_3$ (LAMO-Co) is quite lower than the LAMO.

Acknowledgments

We gratefully acknowledge the support of the Muğla Sıtkı Koçman University Scientific Research Support and Funding Office (BAP) under Grant Contract No: 19/077/01/1/1 for funding this research.

References

1. Adapa SR, Feng T, Ihnfeldt RV, Chen R. Optimisation of a packed particle magnetocaloric refrigerator: A combined experimental and theoretical study. International Journal of Refrigeration, 2024;159:64–73.
2. Kitanovski A. Energy applications of magnetocaloric materials. Adv. Energy Mater., 2020;10:1903741–1903778.
3. Pecharsky VK, Jr. Gschneidner KA. Giant magnetocaloric effect in $Gd_5(Si_2Ge_2)$. Physical Review Letters, 1997;78(23):4494-4497.

4. Khadhraoui S, Baazaoui M, Hsini M, Oumezzine M. Study and modeling of the magnetocaloric effect in the $La_{0.67}Ba_{0.33}Mn_{0.9}Fe_{0.1}O_3$ compound. Journal of Superconductivity and Novel Magnetism, 2019;32:291-300.
5. Pekała M, Drozd V. Magnetocaloric effect in $La_{0.8}Sr_{0.2}MnO_3$ manganite. Journal of Alloys and Compounds, 2008;45:30–33.
6. Çetin SK, Acet M, Güneş M, Ekicibil A, Farle M. Magnetocaloric effect in $(La_{1-x}Sm_x)_{0.67}Pb_{0.33}MnO_3$ ($0 \le x \le 0.3$) manganites near room temperature. Journal of Alloys and Compounds, 2015;650(25):285-294.
7. Mnefgui S, Zaidi N, Dhahri N, Dhahri J, Hlil EK. Electrical transport properties and transport–entropy correlations in $La_{0.57}Nd_{0.1}Sr_{0.33}MnO_3$ manganite. Journal of Magnetism and Magnetic Materials, 2015;384:219-223.
8. Jr. Gschneidner KA, Pecharsky VK, Zimm C. New materials for magnetic refrigeration promise cost effective, environmentally sound air conditioners, refrigerators/freezers, and gas liquefiers. Materials Technology, 1997;12(5-6):145-149.
9. Bruck E. Developments in magnetocaloric refrigeration. J. Phys. D: Appl. Phys., 2005;38:381-391.
10. Pecharsky VK, Jr. Gschneidner KA. Tunable magnetic regenerator alloys with a giant magnetocaloric effect for magnetic refrigeration from ~20 to ~290 K. Appl. Phys. Lett., 1997;70:3299-3301.
11. Xu Y, Memmert U, Hartmann U. Magnetic field sensors from polycrystalline manganites. Sensors and Actuators A: Physical, (2001);91(1–2):26-29.
12. Balevičius S, Novickij J, Abrutis A, Kiprijanovič O, Anisimovas F, Šimkevičius Č, Stankevič V, Vengalis B, Žurauskienė N, Altgilbers LL. Manganite based strong magnetic field sensors used for magnetocumulative generators. Materials Science Forum, 2002;384(38):297–300.
13. Szymczak R, Czepelak M, Kolano R, Kolano-Burian A, Krzymanska B, Szymczak H. Magnetocaloric effect in $La_{1-x}Ca_xMnO_3$ for $x = 0.3$, 0.35, and 0.4. J Mater Sci., 2008;43:1734–1739.
14. Hou DL, Yue CX, Bai Y, Liu QH, Zhao XY, Tang GD. Magnetocaloric effect in $La_{0.8-x}Nd_xNa_{0.2}MnO_3$. Solid State Communications, 2006;140(9–10):459-463.
15. Dinesen AR, Linderoth S, Mørup S. Direct and indirect measurement of the magnetocaloric effect in a $La_{0.6}Ca_{0.4}MnO_3$ ceramic perovskite. Journal of Magnetism and Magnetic Materials, 2002;253:28-34.
16. Jemaa FB, Mahmood S, Ellouze M, Hlil E, Halouani F. Structural, magnetic, and magnetocaloric studies of $La_{0.67}Ba_{0.22}Sr_{0.11}Mn_{1-x}Co_xO_3$ manganites. Journal of Materials Science, 2015;50:620–633.
17. Quintero M, Sacanell J, Ghivelder L, Gomes AM, Leyva AG, Parisi F. Magnetocaloric effect in manganites: metamagnetic transitions for magnetic refrigeration. Appl. Phys. Lett., 2010;97:121916.
18. Kuepper K, Falub MC, Prince KC, Galakhov VR, Troyanchuk IO, Chiuzbaian SG, Matteucci M, Wett D, Szargan R, Ovechkina NA, Mukovskii YaM, Neumann M. Electronic structure of A-site and B-site doped lanthanum manganites: a combined X-ray spectroscopic study. J. Phys. Chem. B, 2005;109(19):9354–9361.

19. Khalyavin DD, Pekala M, Bychkov GI, Shiryaev SV, Barilo SN, Troyanchuk IO, Mucha JM, Szymczak R, Baran M, Szymczak HJ. Magnetotransport properties of flux melt grown single crystals of Co-substituted manganites with perovskite structure. Phys.: Condens. Matter, 2003;15:925.
20. Demeter M, Neumann M, Galakhov VR, Ovechkina NA, Kurmaev EZ, Labachevskaya NI. Electronic structure of doped La-Mn-O perovskites. Acta Physica Polonica A, (2000);98(5):587-591.
21. Klyushnikov OI, Sal'nikov VV, Bogdanovich NM. X-ray photoelectron spectra of $La_{0.7}Ca_{0.3}MnO_3$ and $La_{0.7}Ca_{0.3}Mn_{0.97}Cu_{0.03}O3$ perovskite oxides. Inorg. Mater., 2002;38(3):261–264.
22. Pi L, Zheng L, Zhang Y. Transport mechanism in polycrystalline $La_{0.825}Sr_{0.175}Mn_{1-x}Cu_xO_3$, Phys. Rev. B 2000;61:(13).
23. Zhou HD, Li G, Xu XY, Feng SJ, Qian Y, Li XG. Transport and magnetic properties in $La_{0.7}Ca_{0.3}Mn_{1-x}Cu_xO_3$, Mater. Chem. Phys., 2002;75:140–143.
24. Coşkun A, Irmak AE, Altan B, Ak YS, Coşkun AT. Tuning the magnetic and magnetocaloric properties of a compound via mixing (1–x).$La_{0.67}Ca_{0.33}MnO_3$ +x.$La_{0.67}Sr_{0.33}MnO_3$ (x = 0, 0.25, 0.50, 0.75, 1): composite materials or composite compounds?. Journal of Magnetism and Magnetic Materials, 2023;584:171104.
25. Zhang N, Geng T, Cao HX, Boa JC. Chemical composition and magnetism of Ag doped $LaMnO_3$. Chin. Phys. B, 2008;17:317–322.
26. Tang T, Gu KM, Cao QQ, Wang DH, Zhang SY, Du YW. Magnetocaloric properties of Ag-substituted perovskite-type manganites. J. Magn. Magn. Mater., 2000;222(1-2):110–114.
27. Abozied AET, Ghani AA, Ali AI, Salaheldin TA. Structure, magnetic and magnetocaloric properties of nano crystalline perovskite La0.8Ag0.2MnO3. Journal of Magnetism and Magnetic Materials, 2019;479:260-267.
28. Gamzatov AG, Aliev AM, Batdalov AB, Abdulvagidov ShB, Mel'nikov OV, Gorbenko Oyu. Magnetocaloric effect in silver-doped lanthanum manganites. Technical Physics Letters, 2006;32(6):471–473.
29. Tang T, Gu KM, Cao QQ, Wang DH, Zhang SY, Du YW. Magnetocaloric properties of Ag-substituted perovskite-type manganites. Journal of Magnetism and Magnetic Materials, 2000;222(1–2):110-114.
30. Troyanchuk IO, Lobanovsky LS, Khalyavin DD, Pastushonok SN, Szymczak H. Magnetic and magnetotransport properties of Co-doped manganites with perovskite structure. Journal of Magnetism and Magnetic Materials, 2000;210(1–3):63-72.
31. Kundu AK, Pralong V, Raveau B, Caignaert V. Magnetic and electrical properties of ordered 112-type perovskite $LnBaCoMnO_{5+\delta}$ (Ln = Nd, Eu). J. Mater. Sci., 2011;46:681–687.
32. Chang CL, Tai MF, Chung TW, Lee FY, Su YW, Liu SY, Hwang CS, Tseng PK, Shi JB. X-ray absorption spectroscopy study of the $La_{0.7}Ba_{0.3}Mn_{1-x}Co_xO_3$ system. Journal of Magnetism and Magnetic Materials, 2000;209(1–3):240-242.